World Journal of Biology Pharmacy and Health Sciences
eISSN: 2582-5542
Cross Ref DOI: 10.30574/wjbphs
Journal homepage: https://wjbphs.com/

(Research Article)

Check for updates

Detection of hotspots and coldspots of the incidence of hand, foot and mouth diseases: A case study in Ho Chi Minh city, Vietnam

Bui Thi Cham and Nguyen Thi Quynh Trang *

Faculty of Nursing, Phenikaa University, Hanoi 12116, Vietnam.

World Journal of Biology Pharmacy and Health Sciences, 2024, 19(02), 527–535

Publication history: Received on 15 July 2024; revised on 25 August 2024; accepted on 28 August 2024

Article DOI: https://doi.org/10.30574/wjbphs.2024.19.2.0549

Abstract

Background: Hand, foot, and mouth disease (HFMD) is a common pediatric illness mostly caused by Coxsackievirus A16 (CV-A16) and Human Enterovirus 71 (EV-A71). HFMD has grown significantly over the last 20 years, and it has drawn a lot of attention. To better understand of the epidemiology of HFMD, this study aims to investigate the use of Getis-Ord's G_i^* statistic in the identification of hotspots and coldspots of HFMD in Ho Chi Minh city, Vietnam.

Methods: Getis-Ord's G_i^* statistic was first applied to identify hotspots and coldspots of HFMD incidence including high-high, low-low spatial clusters. HFMD cases and infection rates collected in Ho Chi Minh were then used to explore the spatial clusters of HFMD Finally, the main findings will be discussed and summarised.

Results: It was found that the large number of hand, foot and mouth disease cases were mainly concentrated in the western area of Ho Chi Minh City. A total of 04 hotspot clusters and 05 coldspots of HFMD infection rate were detected in the 29th week of 2024 in the west, center and north of Ho Chi Minh City, respectively. Whereas, 06 hotspots and 04 coldspots of HFMD infection rate were detected in the 30th week of 2024 in the west, south and center of Ho Chi Minh City, respectively.

Conclusions: The results of this investigation confirm the value of Getis-Ord's G_i^* statistic in the detection of hotspots and coldspots associated with confirmed cases of HFMD.

Keywords: Getis-Ord's statistic; Hotspots; Coldspots; Spatial distribution, Hand; Foot and mouth diseases; Ho Chi Minh city, Vietnam

1. Introduction

Hand, foot and mouth illness (HFMD) has gotten to be an endemic childhood infection. Its fundamental etiologic operators are human enterovirus 71 (EV-A71) and Coxsackievirus 16 (CV-A16) (1). As early as 1957, the characteristic indications of fever, vesicular hasty on hands and feet caused by Coxsackievirus (CV), essentially CVA16, was to begin with detailed in Toronto (2,3). In the last few decades, reports of HFMD epidemics worldwide attributed to Enterovirus A71 (EV-A71), CVA16, CVA6, and Echoviruses (Echo) have been commonplace (4). The symptoms of HFMD sickness were fever, a rash resembling blisters on the hands and feet, and oral ulcers brought on by burst blisters in the mouth. The condition was generally minor and typically lasted less than a week (5). Globally, HFMD outbreaks have been documented, and within the past ten years, Western Pacific countries have seen numerous HFMD epidemics (6–9). HFMD poses a risk to public health in Asia, specifically in Singapore(10,11), Malaysia (11,12), Japan (13) and Vietnam (14–16). Numerous studies have been reported that HFMD has grown to be a serious public health issue in the Asia-Pacific area and beyond (17).

* Corresponding author: Nguyen Thi Quynh Trang; Email: trang.nguyenthiquynh@phenikaa-uni.edu.vn

Geographical places are the subject of HFMD-related data since they are a kind of spatial object with a spatial dimension. Spatial statistics are a useful tool for studying epidemiological data such as HFMD (18). A crucial tool for analyzing the spatial pattern of spatial objects is a spatial statistic (19). In accordance with Tobler's First Law of Geography, epidemiological research have effectively used commonly used statistics for spatial auto-correlation analysis, such as global spatial statistics (Moran's I, Getis-Ord G* and Geary's C) and local indicators of spatial association (LISA) (20–23) in general, and in the investigation of COVID-19's transmission (24–26) and HFMD (27,28) in particular. Spatial statistics, for instance, were used in a study on the spatiotemporal analysis and hotspot detection of COVID-19 in southern, northern, and western Europe (29). The spatiotemporal COVID-19 spread over Oman was studied using the local Moran's I autocorrelation coefficient, Getis-Ord General-G high/low clustering, and Getis-Ord's statistic (30). Spatial analysis has been widely used in HIV/AIDS research, aside from the applications of Getis-Ord's statistic on HFMD studies, to identify high-risk and spatiotemporal clusters, evaluate the geographic distribution of infections, and investigate the spatial relationship between HIV/AIDS and social factors (31,32). Understanding the long-term patterns and spatial clustering of HIV/AIDS cases can be accomplished with the help of spatial analysis. Policymakers and public health experts can use spatial analysis to acquire scientific viewpoints for creating focused countermeasures (33). Furthermore, geographic information systems (GIS) and other geospatial analytical techniques are crucial for comprehending the nature and reasons behind regional variations in HIV prevalence (34). However, there are still very few geographically explicit studies on HIV/AIDS in sub-Saharan Africa, despite the notable increase in the use of such geospatial tools in understanding public health problems, designing and executing treatments, and assessing their effectiveness (35,36).

Controlling hand, foot, and mouth infections heavily depends on knowledge about the spatial distribution, hotspots, and coldspots of HFMD confirmed cases. Thus, this study was conducted to identify hotspots and coldspots of HFMD using Getis-Ord's G_i^* statistic collected in the final two weeks of July 2024 in Ho Chi Minh City, Vietnam. The Getis-Ord's G_i^* statistic is then employed to measure spatial auto-correlation between the incidence of HFMD confirmed cases, and then identify hotspots and coldspots of HMFD cases. Spatial distribution of these hotspots and coldspots will be mapped with the help of a GIS. Finally, the main findings will be discussed and summarised.

2. Data used and methods

2.1. Data used

An HFMD outbreak occurred in 2023 Ho Chi Minh City. Districts of 6, 8, 12, Tan Phu, Binh Tan, and Binh Chanh had high incidence rates of HFMD illnesses per 100,000 people (37). The health department of Ho Chi Minh City reports that the HFMD pandemic has grown quickly and could continue for an additional three to four months after August 2023. In particular, the second peak of the HFMD outbreak will fall around the time that students return to school. According to reports, the city saw 1,614 HFMD cases, which is a concerning increase of about 2.5 times when compared to the average of 716 instances that were reported four weeks prior (37). In this study, a datasets of HFMD cases and HFMD incidence were collected in Ho Chi Minh City collected in the last 2 weeks of July 2024 in Ho Chi Minh City to investigate the use of Getis-Ord's G_i^* statistic in the identification of hotspots and coldspots of HFMD in Ho Chi Minh city, Vietnam.

2.2. Methods

The degree to which a variable is linked with itself spatially is expressed by spatial autocorrelation. Tobler's First Law of Geography, which asserts that "everything is related to everything else, but near things are more related than distant things" (38). One of the core ideas of spatial analysis is spatial autocorrelation (39). It deviates from the independent observation assumption of classical statistics by describing the correlation among values of a single variable that is only attributable to their relatively close locational positions on a two-dimensional surface (40). When a variable exhibits positive spatial autocorrelation, its values that are geographically close to one another on a map tend to be similar: high values are typically found close to high values, medium values are close to medium values, and low values are close to low values. When data with similar values are clustered together, there is positive spatial autocorrelation. When observations with different values are closer together, negative spatial autocorrelation takes place (i.e., scattered). In a regression model, spatial autocorrelation can be measured by adding an autoregressive parameter, indexed, or filtered out of variables. Indices are a useful tool for quantifying spatial autocorrelation. Indexes that condense the degree to which comparable observations tend to occur close to one another across the study region can be used to evaluate spatial autocorrelation. Two common indices that are used to assess spatial autocorrelation in areal data are Moran's I statistic (41) and Getis-Ord's G_i^* statistic (42).

Spatial autocorrelation and cluster analysis are two techniques for examining spatial trends and identifying hotspots (43). An location with a higher concentration of occurrences than would be predicted from a random distribution of events is called a hotspot (44). The past few decades have seen a significant increase in the use of hotspot analysis in public health and epidemiological research, as well as in other disciplines (for example, crime mapping and research contribute significantly to the literature on hotspot analysis). This increase has been primarily attributed to the development of Geographic Information Systems (GIS)-based software (45–47). The examination of spatial autocorrelation examines the degree of similarity between values that are closer to one another (48). Global and local indications of spatial connection can be identified using spatial autocorrelation measurements (21). The incidence rates were subjected to spatial autocorrelation analysis in order to determine if the cases were dispersed randomly throughout space and, if not, to assess the statistical significance of any spatial illness clusters that were found (49). A circumstance suggesting a type of clustering in a spatial distribution is called a hotspot (49). Hotspot analysis is based on the Getis-Ord's G_i^* statistic. By examining each feature in relation to its surrounding characteristics, hotspot analysis characterizes the presence of hotspots (high clustered values) and coldspots (low clustered values) over a given area (44). Hotspot can distinguish between high- and low-value clusters. It is, therefore, the counties with the highest and lowest numbers of HFMD confirmed cases were determined using the Getis-Ord's G_i^* statistic (18,50). The form of Getis-Ord's G_i^* statistic is defined as follows (51):

$$G_i^* = \frac{\sum_{j=1}^{N} W_{ij}\, x_j - \overline{x} \sum_{j=1}^{N} W_{ij}}{S\sqrt{\frac{N\sum_{j=1}^{N}[W_{ij}^2 - (W_{ij})^2]}{N-1}}} \quad \text{..........................(1)}$$

with:

$$\overline{x} = \frac{1}{N}\sum_{j=1}^{N} x_j \quad \text{..................(2)}$$

and:

$$S = \sqrt{\frac{\sum_{j=1}^{N} x_j^2}{N} - (\overline{x})^2} \quad \text{......................(3)}$$

Expectation:

$$\mathrm{E}(\mathrm{G_i^*}) = \frac{\mathrm{W}_i^*}{\mathrm{n}-1} \quad \text{.....................(4)}$$

with:

$$\mathrm{W}_i^* = \sum_{j=1}^{\mathrm{n}} \mathrm{w}_{ij}(d) \quad \text{..........................(5)}$$

and variance:

$$\mathrm{Var}(\mathrm{G_i^*}) = \frac{\mathrm{W}_i^*(\mathrm{n}-\mathrm{W}_i^*)\mathrm{Y}_{i2}^*}{\mathrm{n}^2(\mathrm{n}-1)(\mathrm{Y}_{i1}^*)^2} \quad \text{........................(6)}$$

with:

$$\mathrm{Y}_{i1}^* = \frac{\sum_{j=1}^{\mathrm{n}} \mathrm{x_j}}{\mathrm{n}}; \quad \text{..........................(7)}$$

and:

$$\mathrm{Y}_{i2}^* = \frac{\sum_{i=1}^{\mathrm{n}}\sum_{j=1}^{\mathrm{n}}\left(\mathrm{x_i x_j}\right)^2}{\mathrm{n}} - (\mathrm{Y}_{i1}^*)^2; \quad \text{........................(8)}$$

where: the Getis-Ord's G_i^* statistic is computed for the number of HFMD confirmed cases at county i; x_i, x_j, $\bar{x}$, and W_{ij} are defined in equation (1); and N is the total number of neighborhood counties as defined in equation (2). W_{ij} can be constructed using the methods of the first order and second of contiguity. In this study, adjacency to compute W_{ij} is defined using the first order of continuity.

The Getis-Ord's G_i^* coefficient at county i (G_i^*) varies from -1 to +1. If $G_i^* > 0$ and $p(G_i^*) < \alpha$ then A high-high value spatial clustering is present (18,50). In this case, these extremely high readings, also referred to as "hotspots," indicate the existence of a large number of HFMD confirmed case among county i and its neighborhood counties ($j \in J_i$). Whereas, if $G_i^* < 0$ and $p(G_i^*) < \alpha$ then a low-low value spatial clustering is present (18,50). These extremely low scores are referred to as "coldspots," signifying a dearth of confirmed cases of HFMD among county i and its neighborhood counties ($j \in J_i$). If the value of G_i^*close zero and $p(G_i^*) < \alpha$ then there will be neither hotspots nor coldspots or random distribution of

HFMD confirmed cases (50). Random clusters of cases can also affect how quickly an infectious disease spreads (49). The output from Getis-Ord's G_i^* statistic identifies spatial clusters of high values (hotspots) and spatial clusters of low values (cold spots). If the dataset has a highly skewed distribution, the test is not successful. It is, therefore, testing for the significance of the Getis-Ord's G_i^* statistic in this study was also carried out by a randomization test using 999 permutations. In this work, with the help of the spatial statistics software, GeoDA, developed by (52), The test for the spatial autocorrelation statistics was examined using a randomization test. 999 permutations were used to create and test spatial auto-correlation statistics at the significance level of 0.05. The null hypothesis can be rejected when the p-value is extremely little since it indicates that there is a very small probability (small likelihood) that the observed spatial pattern is the product of random processes (49).

3. Results and discussion

3.1. Spatial distribution of the incidence of HFMD confirmed cases

Data from Map in Figure 1 shows the spatial distribution of the incidence of HFMD confirmed cases in the last 2 weeks of July 2024 in Ho Chi Minh City. The spatial distribution of the incidence of HFMD confirmed cases collected in the 27th week of 2024 is divided into five ranges: very low (less than 55 cases/100,000 people), low (from 55 cases/100,000 people to 72 cases/100,000 people), medium (from 72 cases/100,000 people to 87 cases/100,000 people), high (from 87 cases/100,000 people to 134.2 cases/100,000 people) and very high (from 134.2 cases/100,000 people to 142 cases/100,000 people). It can be seen from the spatial distribution of hand, foot and mouth disease cases in Figure 1 (left) that the large number of hand, foot and mouth disease cases were mainly concentrated in the western area of Ho Chi Minh City, typically in Binh Chanh (142 cases/100,000 people) and Nha Be (137 cases/100,000 people). The average infection rate was distributed in the eastern and northern areas of the city such as Cu Chi (89 cases/100,000 people), Thu Duc (87 cases/100,000 people) and Binh Tan (122 cases/100,000 people). The low infection rate is concentrated in the central and southern areas of the city, typically Phu Nhuan (55 cases/100,000 people), Hoc Mon (72 cases/100,000 people), District 3 (72 cases/100,000 people) and Can Gio (78 cases/100,000 people).

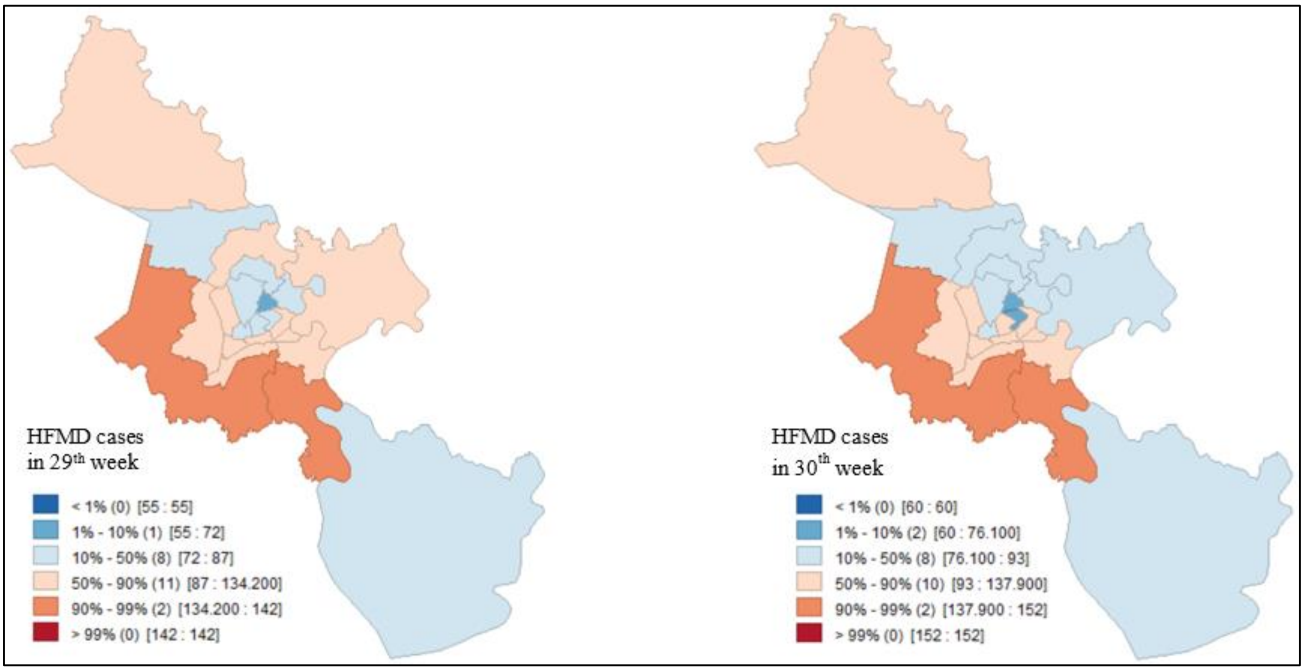

Figure 1 Spatial distribution of the incidence of hand, foot and mouth diseases in Ho Chi Minh city, Vietnam.

The spatial distribution of the incidence of HFMD cases collected in 30th week of 2024 is shown in Figure 1 (right) and is also classified into five ranges: very low (less than 60 cases/100,000 people), low (from 60 cases/100,000 people to 76.1 cases/100,000 people), medium (from 76.1 cases/100,000 people to 93 cases/100,000 people), high (from 93 cases/100,000 people to 137.9 cases/100,000 people) and very high (from 137.9 cases/100,000 people to 152 cases/100,000 people). It can be seen from the spatial distribution map of hand, foot and mouth disease cases in Figure 1 (right) that, in this week, the large number of hand, foot and mouth disease cases was still mainly concentrated in the western area of Ho Chi Minh city, typically in Binh Chanh (152 cases/100,000 people) and Nha Be (140 cases/100,000 people). The average infection rate was distributed in the eastern, northern and surrounding areas of the city center such as Thu Duc (97 cases/100,000 people), Cu Chi (93 cases/100,000 people), Tan Phu (93 cases/100,000 people) and District 1 (93 cases/100,000 people). The low infection rate this week is still concentrated in the central and southern areas of the city, typically Phu Nhuan (60 cases/100,000 people), District 3 (74 cases/100,000 people) or Hoc Mon (77 cases/100,000 people).

3.2. Analysis of spatial distribution of hotspots and coldspots of HFMD incidence

The results of hotspot identification from the HFMD infection rate in Ho Chi Minh City for the 29th week of 2024 are shown in Figure 2. Data from the Getis-Ord cluster map Figure 2-left shows that a total of 04 hotspot clusters and 05 coldspots of HFMD infection rate were detected in the west, center and north of Ho Chi Minh City, respectively. Specifically, 04 hotspot clusters were detected in districts with the following corresponding infection rates: Binh Chanh (142 cases/100,000 people), Binh Tan (122 cases/100,000 people), District 8 (133 cases/100.000 people) and District 7 (103 cases/100 people). Five coldspot clusters were detected in Cu Chi (93 cases/100,000 people), Tan Binh (84 cases/100,000 people), Go Vap (82 cases/100,000 people), Phu Nhuan (55 cases/100,000 people) and District 1 (90 cases/100,000 people). Some districts had high infection rates but no hotspots detected, such as Nha Be (137 cases/100,000 people) or District 6 (118 cases/100,000 people). Meanwhile, some districts have low infection rates but no coldspots detected, such as District 3 (72 cases/100,000 people) or Can Gio and Go Vap (78 cases/100,000 people). Data from Figure 2-right shows the spatial distribution of statistical significance (p-value) achieved by the local Getis-Ord index for each district in Ho Chi Minh City. The statistical significance levels are shown on a 4-point scale from not achieving statistical significance (p-value > 0.05) and achieving statistical significance at levels 0.05, 0.01 and 0.001. Data from Figure 2 (right) shows that there are local Getis-Ord indexes achieving significance at level 0.05 detected in the central and northern districts of the city such as Cu Chi, Binh Tan, Go Vap, Phu Nhuan and District 1. Meanwhile, Binh Chanh, District 8, District 7 and Tan Binh.

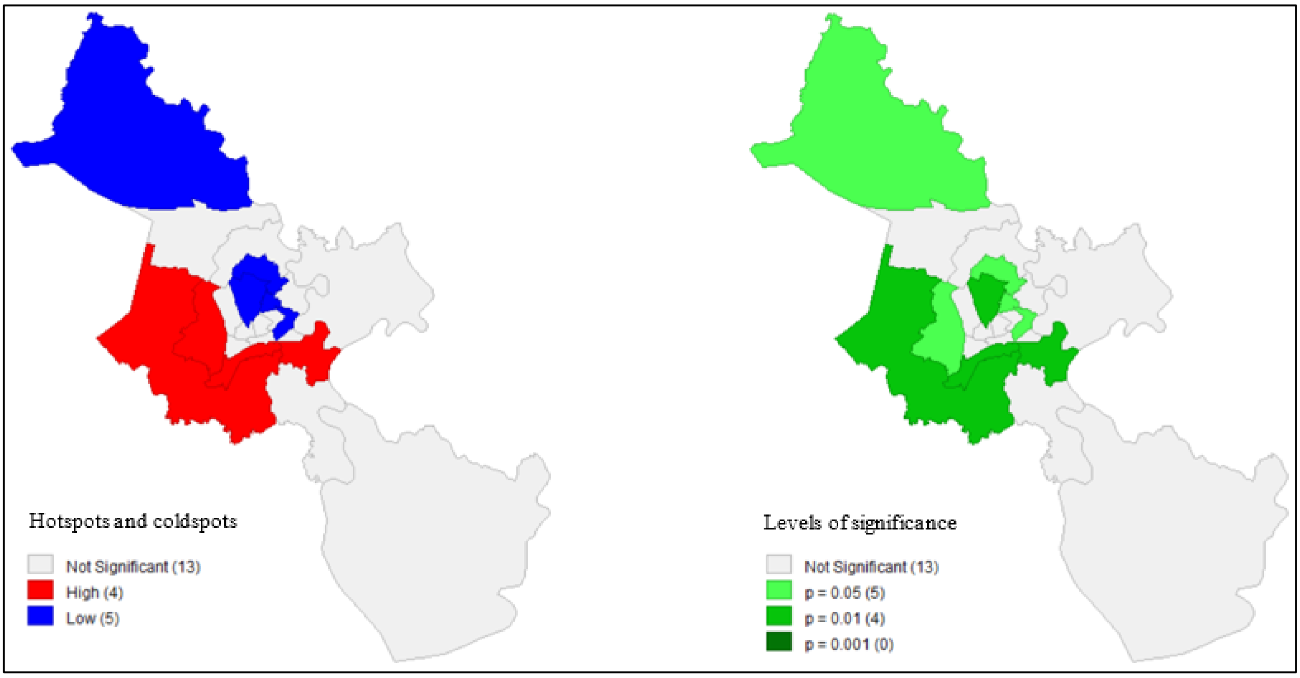

Figure 2 Spatial distribution of hotspots and coldspots (left) and significant (right) maps of HFMD confirmed cases in the 29th week in 2024 in Ho Chi Minh city, Vietnam.

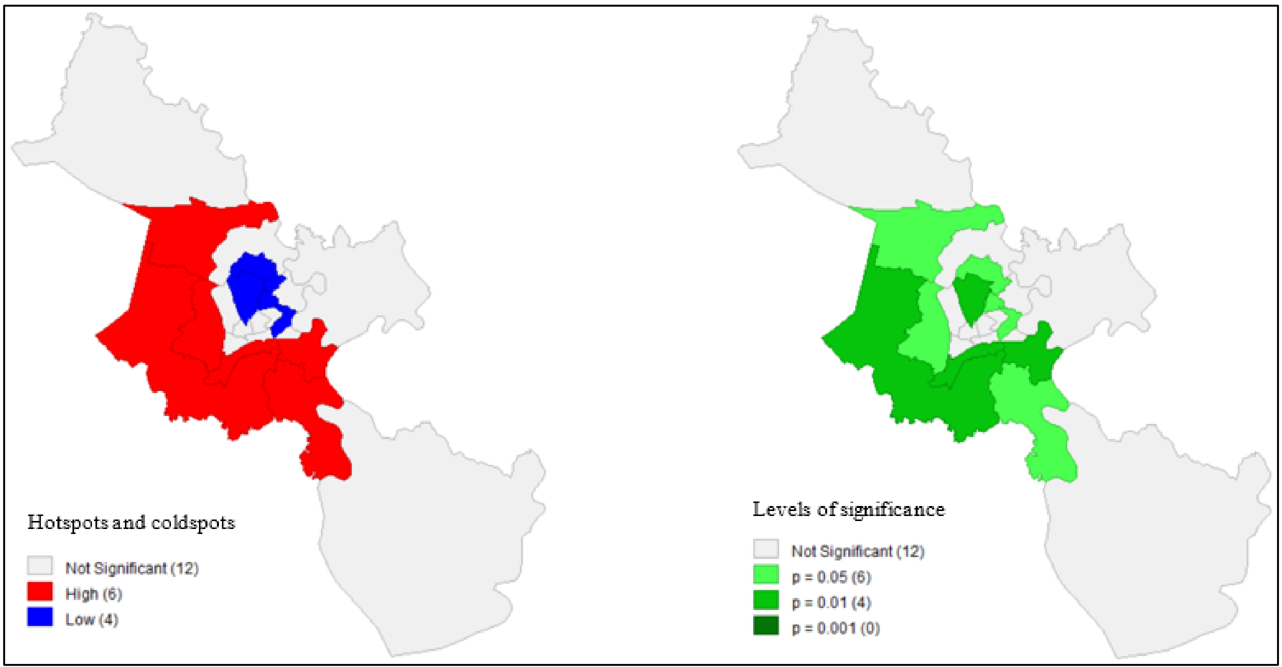

Figure 3 Spatial distribution of hotspots and coldspots (left) and significant (right) maps of HFMD confirmed cases in the 30th week in 2024 in Ho Chi Minh city, Vietnam.

The dentification of hotspot obtained from the HFMD infection rate in Ho Chi Minh City for the 30th week of 2024 are shown in Figure 3. Data from the Getis-Ord cluster map Figure 3-left shows that a total of 06 hotspots and 04 coldspots of HFMD infection rate were detected in the west, south and center of Ho Chi Minh City, respectively. Specifically, 06 hotspot clusters were detected in the western and southwestern districts of the city with the corresponding infection rates as follows: Hoc Mon (77 cases/100,000 people), Binh Chanh (152 cases/100,000 people), Binh Tan (128 cases/100,000 people), District 8 (137 cases/100,000 people), District 7 (106 cases/100,000 people) and Nha Be (140 cases/100,000 people). Some districts have high infection rates but no hotspots are detected such as District 6 (123 cases/100,000 people) and District 5 (99 cases/100,000 people). Four coldspot clusters were detected in the city center, namely in Go Vap (82 cases/100,000 people), Tan Binh (84 cases/100,000 people), Phu Nhuan (60 cases/100,000 people) and District 11 (93 cases/100,000 people). Meanwhile, some districts with low infection rates did not detect coldspots, such as District 3 (72 cases/100,000 people) or Can Gio and Go Vap (78 cases/100,000 people). Data from Figure 3-right shows the spatial distribution of statistical significance (p-value) achieved by the local Getis-Ord index for each district in Ho Chi Minh City in the 30th week of 2024. The statistical significance levels are also presented on a 4-point scale from not reaching statistical significance (p-value > 0.05) to reaching statistical significance at the levels of 0.05, and 0.01. Data from Figure 3 (right) show that there are local Getis-Ord indices reaching the significance level at the 0.05 level detected in the central districts of the city such as Hoc Mon, Go Vap, Phu Nhuan, and District 1. Meanwhile, Binh Chanh, District 8, Tan Binh, and District 7.

4. Conclusion

This study aims to investigate the use of Getis-Ord's G_i^* statistic in the identification of hotspots and coldspots of HFMD in Ho Chi Minh city, Vietnam. Getis-Ord's G_i^* statistic was first applied to identify hotspots and coldspots of HFMD incidence including high-high, low-low spatial clusters. HFMD cases and infection rates collected in Ho Chi Minh were then used to explore the spatial clusters of HFMD Finally, the main findings will be discussed and summarised. Study results show that the large number of hand, foot and mouth disease cases were mainly concentrated in the western area of Ho Chi Minh City. A total of 04 hotspot clusters and 05 coldspots of HFMD infection rate were detected in the 29th week of 2024 in the west, center and north of Ho Chi Minh City, respectively. Whereas, 06 hotspots and 04 coldspots of HFMD infection rate were detected in the 30th week of 2024 in the west, south and center of Ho Chi Minh City, respectively. In summary, this study's findings support the usefulness of Getis-Ord's G_i^* statistic for identifying hotspots and coldspots associated to HFMD confirmed cases.

Compliance with ethical standards

Acknowledgments

The authors would like to thank Center for Disease Control of Ho Chi Minh City for providing the data and the anonymous reviewers for their careful reading of our manuscript and their many insightful comments and suggestions

Disclosure of conflict of interest

The authors declare no conflict of interest.

Statement of ethical approval

Ethical approval approved.

Statement of informed consent

Informed consent was obtained from all individual participants included in the study.

References

[1] Koh WM, Bogich T, Siegel K, Jin J, Chong EY, Tan CY, et al. The epidemiology of hand, foot and mouth disease in Asia: a systematic review and analysis. Pediatr Infect Dis J. 2016;35(10):e285.

[2] Robinson CR, Doane FW, Rhodes AJ. Report of an outbreak of febrile illness with pharyngeal lesions and exanthem: Toronto, summer 1957—isolation of group A coxsackie virus. Can Med Assoc J. 1958;79(8):615.

[3] Clarke M, Hunter M, McNAUGHTON GA, Von Seydlitz D, Rhodes AJ. Seasonal aseptic meningitis caused by Coxsackie and ECHO viruses, Toronto, 1957. Can Med Assoc J. 1959;81(1):5.

[4] Bubba L, Broberg EK, Jasir A, Simmonds P, Harvala H, Redlberger-Fritz M, et al. Circulation of non-polio enteroviruses in 24 EU and EEA countries between 2015 and 2017: a retrospective surveillance study. Lancet Infect Dis. 2020;20(3):350–61.

[5] Alsop J, Flewett TH, Foster JR. "Hand-foot-and-mouth disease" in Birmingham in 1959. Br Med J. 1960;2(5214):1708.

[6] Ang LW, Koh BK, Chan KP, Chua LT, James L, Goh KT. Epidemiology and control of hand, foot and mouth disease in Singapore. Ann Acad Med Singapore. 2009;38(2):106–12.

[7] Chatproedprai S, Theanboonlers A, Korkong S, Thongmee C, Wananukul S, Poovorawan Y. Clinical and molecular characterization of hand-foot-and-mouth disease in Thailand, 2008–2009. Jpn J Infect Dis. 2010;63(4):229–33.

[8] Bo Y-C, Song C, Wang J-F, Li X-W. Using an autologistic regression model to identify spatial risk factors and spatial risk patterns of hand, foot and mouth disease (HFMD) in Mainland China. BMC Public Health. 2014;14(1):1–13.

[9] Österback R, Vuorinen T, Linna M, Susi P, Hyypiä T, Waris M. Coxsackievirus A6 and hand, foot, and mouth disease, Finland. Emerg Infect Dis. 2009;15(9):1485.

[10] Shah VA, Chong CY, Chan KP, Ng W, Ling AE. Clinical characteristics of an outbreak of hand, foot and mouth disease in Singapore. Ann Acad Med Singapore. 2003;32(3):381–7.

[11] McMinn P, Lindsay K, Perera D, Chan HM, Chan KP, Cardosa MJ. Phylogenetic analysis of enterovirus 71 strains isolated during linked epidemics in Malaysia, Singapore, and Western Australia. J Virol. 2001;75(16):7732–8.

[12] AbuBakar S, Chee H-Y, Al-Kobaisi MF, Xiaoshan J, Chua KB, Lam SK. Identification of enterovirus 71 isolates from an outbreak of hand, foot and mouth disease (HFMD) with fatal cases of encephalomyelitis in Malaysia. Virus Res. 1999;61(1):1–9.

[13] Onozuka D, Hashizume M. The influence of temperature and humidity on the incidence of hand, foot, and mouth disease in Japan. Sci Total Environ. 2011;410:119–25.

[14] Nhan LNT, Khanh TH, Hong NTT, Van HMT, Nhu LNT, Ny NTH, et al. Clinical, etiological and epidemiological investigations of hand, foot and mouth disease in southern Vietnam during 2015–2018. PLoS Negl Trop Dis. 2020;14(8):e0008544.

[15] Nguyen NTB, Pham H V, Hoang CQ, Nguyen TM, Nguyen LT, Phan HC, et al. Epidemiological and clinical characteristics of children who died from hand, foot and mouth disease in Vietnam, 2011. BMC Infect Dis. 2014;14:1–7.

[16] Anh NT, Van HMT, Hong NTT, Thanh TT, Hang VTT, Ny NTH, et al. Emerging coxsackievirus A6 causing hand, foot and mouth disease, Vietnam. Emerg Infect Dis. 2018;24(4):654.

[17] Zhu P, Ji W, Li D, Li Z, Chen Y, Dai B, et al. Current status of hand-foot-and-mouth disease. J Biomed Sci. 2023;30(1):15.

[18] Hoang A, Nguyen T. Identifying Spatio-Temporal Clustering of the COVID-19 Patterns Using Spatial Statistics: Case Studies of Four Waves in Vietnam. Int J Appl Geospatial Res. 2022;13(1):1–15.

[19] Kieu Q-L, Nguyen T-T, Hoang A-H. GIS and remote sensing: a review of applications to the study of the COVID-19 pandemic. Geogr Environ Sustain. 2021;14(4).

[20] Gonzalez-Rubio J, Najera A, Arribas E. Comprehensive personal RF-EMF exposure map and its potential use in epidemiological studies. Environ Res. 2016;149:105–12.

[21] Fecht D, Hansell AL, Morley D, Dajnak D, Vienneau D, Beevers S, et al. Spatial and temporal associations of road traffic noise and air pollution in London: Implications for epidemiological studies. Environ Int. 2016;88:235–42.

[22] Alves JD, Abade AS, Peres WP, Borges JE, Santos SM, Scholze AR. Impact of COVID-19 on the indigenous population of Brazil: A geo-epidemiological study. Epidemiol Infect. 2021;149:e185.

[23] Şener R, Türk T. Spatiotemporal analysis of cardiovascular disease mortality with geographical information systems. Appl Spat Anal Policy. 2021;14(4):929–45.

[24] Xie Z, Qin Y, Li Y, Shen W, Zheng Z, Liu S. Spatial and temporal differentiation of COVID-19 epidemic spread in mainland China and its influencing factors. Sci Total Environ. 2020;744:140929.

[25] Aral N, Bakır H. Spatiotemporal pattern of Covid-19 outbreak in Turkey. GeoJournal. 2023;88(2):1305–16.

[26] Zhang P, Yang S, Dai S, Aik DHJ, Yang S, Jia P. Global spreading of Omicron variant of COVID-19. Geospat Health. 2022;17(s1).

[27] Nguyen HX, Chu C, Nguyen HLT, Nguyen HT, Do CM, Rutherford S, et al. Temporal and spatial analysis of hand, foot, and mouth disease in relation to climate factors: a study in the Mekong Delta region, Vietnam. Sci Total Environ. 2017;581:766–72.

[28] Deng T, Huang Y, Yu S, Gu J, Huang C, Xiao G, et al. Spatial-temporal clusters and risk factors of hand, foot, and mouth disease at the district level in Guangdong Province, China. PLoS One. 2013;8(2):e56943.

[29] Shariati M, Mesgari T, Kasraee M, Jahangiri-Rad M. Spatiotemporal analysis and hotspots detection of COVID-19 using geographic information system (March and April, 2020). J Environ Heal Sci Eng. 2020;18:1499–507.

[30] Al-Kindi KM, Alkharusi A, Alshukaili D, Al Nasiri N, Al-Awadhi T, Charabi Y, et al. Spatiotemporal assessment of COVID-19 spread over Oman using GIS techniques. Earth Syst Environ. 2020;4:797–811.

[31] Liu H, Lin X, Xu Y, Chen S, Shi J, Morisky D. Emerging HIV epidemic among older adults in Nanning, China. AIDS Patient Care STDS. 2012;26(10):565–7.

[32] Lu L, Jia M, Ma Y, Yang L, Chen Z, Ho DD, et al. The changing face of HIV in China. Nature. 2008;455(7213):609–11.

[33] Yuan F, Liu L, Liu L, Zeng Y, Zhang L, He F, et al. Epidemiological and spatiotemporal analyses of HIV/AIDS prevalence among older adults in Sichuan, China between 2008 and 2019: A population-based study. Int J Infect Dis. 2021;105:769–75.

[34] Zulu LC, Kalipeni E, Johannes E. Analyzing spatial clustering and the spatiotemporal nature and trends of HIV/AIDS prevalence using GIS: the case of Malawi, 1994-2010. BMC Infect Dis. 2014;14(1):1–21.

[35] Tanser F, Bärnighausen T, Cooke GS, Newell M-L. Localized spatial clustering of HIV infections in a widely disseminated rural South African epidemic. Int J Epidemiol. 2009;38(4):1008–16.

[36] Kalipeni E, Zulu L. Using GIS to model and forecast HIV/AIDS rates in Africa, 1986–2010. Prof Geogr. 2008;60(1):33–53.

[37] VietNamNews. HCM City faces burden of hand, foot, mouth disease and dengue fever [Internet]. Available from: https://vietnamnews.vn/society/1551273/hcm-city-faces-burden-of-hand-foot-mouth-disease-and-dengue-fever.html

[38] Tobler W. On the first law of geography: A reply. Ann Assoc Am Geogr. 2004;94(2):304–10.

[39] Getis A. A history of the concept of spatial autocorrelation: A geographer's perspective. Geogr Anal. 2008;40(3):297–309.

[40] Mauricio Bini L, Diniz-Filho JAF, Rangel TF, Akre TSB, Albaladejo RG, Albuquerque FS, et al. Coefficient shifts in geographical ecology: an empirical evaluation of spatial and non-spatial regression. Ecography (Cop). 2009;32(2):193–204.

[41] Anselin L. Local indicators of spatial association—LISA. Geogr Anal. 1995;27(2):93–115.

[42] Geary RC. The contiguity ratio and statistical mapping. Inc Stat. 1954;5(3):115–46.

[43] Elliott P, Wartenberg D, Marshall RJ, Rosli NM, Shah SA, Mahmood MI, et al. A review of methods for the statistical analysis of spatial patterns of disease. J R Stat Soc Ser A (Statistics Soc. 2021;154(1):998–1006.

[44] Nguyen TT, Vu TD. Use of hot spot analysis to detect underground coal fires from landsat-8 TIRS data: A case study in the Khanh Hoa coal field, North-East of Vietnam. Environ Nat Resour J. 2019;17(3).

[45] Murad A, Khashoggi BF. Using GIS for disease mapping and clustering in Jeddah, Saudi Arabia. ISPRS Int J Geo-Information. 2020;9(5):328.

[46] Gao S, Mioc D, Anton F, Yi X, Coleman DJ. Online GIS services for mapping and sharing disease information. Int J Health Geogr. 2008;7:1–12.

[47] Rican S, Salem G. Mapping disease. A companion to Heal Med Geogr. 2009;14:96.

[48] Vu D-T, Nguyen T-T. Spatial pattern of land surface temperatures and its relation to underground coal fires in the Khanh Hoa Coal Field, North-East of Vietnam. Arab J Geosci. 2021;14(3).

[49] Kulldorff M, Feuer EJ, Miller BA, Freedma LS. Breast cancer clusters in the northeast United States: a geographic analysis. Am J Epidemiol. 1997;146(2):161–70.

[50] Vu D-T, Nguyen T-T, Hoang A-H. Spatial clustering analysis of the COVID-19 pandemic: A case study of the fourth wave in Vietnam. Geogr Environ Sustain. 2021;14(4).

[51] Cliff AD, Ord JK. Spatial processes: models & applications. (No Title). 1981

[52] Anselin L, Syabri I, Kho Y. GeoDa: an introduction to spatial data analysis. In: Handbook of applied spatial analysis: Software tools, methods and applications. Springer; 2009. p. 73–89.